INVESTIGATION OF ROTATING STALL IN A CENTRIFUGAL VANED DIFFUSER

Frank Tafe Hemler
and
Calvin Yuke Sing

Letter on front cover:

INVESTIGATION OF ROTATING STALL

IN A CENTRIFUGAL VANED DIFFUSER

Frank Tafe Hemler
and
Calvin Yuke Sing

Cambridge, Massachusetts
May 24, 1954

Professor L. F. Hamilton
Secretary of the Faculty
Massachusetts Institute of Technology
Cambridge, Massachusetts

Dear Sir:

In partial fulfillment of the requirements for the degree of Master of Science in Aeronautical Engineering, we herewith submit a thesis entitled "Investigation of Rotating Stall in a Centrifugal Vaned Diffuser".

INVESTIGATION OF ROTATING STALL IN A CENTRIFUGAL VANED DIFFUSER

by

FRANK TAFE HEMLER
B.S.A.E., United States Naval Postgraduate School
(1953)

and

CALVIN YUKE SING
B. E., University of Toledo
(1948)

SUBMITTED IN PARTIAL FULFILLMENT
OF THE REQUIREMENTS FOR THE
DEGREE OF MASTER OF
SCIENCE

at the

MASSACHUSETTS INSTITUTE OF TECHNOLOGY
May 1954

INVESTIGATION OF ROTATING STALL IN A CENTRIFUGAL VANED DIFFUSER

by

FRANK E. HEMLER, LT. U.S. NAVY

and

CALVIN Y. SING

Submitted to the Department of Aeronautical Engineering on 24 May 1954 in partial fulfillment of the requirements for the degree of Master of Science in Aeronautical Engineering.

SUMMARY

There is a definite need for information on rotating stall. Although some investigations have been made on cascades and axial compressors, very few investigations have been made with centrifugal compressors. Further, the present theory concerning the causes of rotating stall are still somewhat nebulous. Therefore, investigations were carried out with a centrifugal vaned diffuser.

The flow in the centrifugal vaned diffuser was studied with barium titanate crystals and tufts. The mass flow, pressure, velocity, solidity factor, angle of attack and blade types were varied in the test section in order to obtain as much information as possible.

No rotating stall was encountered at any of the conditions investigated. Due to the results of these experiments, it was decided that the present theory is incomplete. Recommended future investigations should include:

(1) A dimensional analysis attack on the problem.

(2) The study of the flow in a centrifugal diffuser with flat plates. Each plate should be out of the stalled region of adjacent plates.

(3) The study of rotating stall as produced by the British in one of the references.

(4) The further study of the flow in a centrifugal compressor with blades of gentle stall characteristics.

These investigations were accomplished by two graduate students, Lt. Frank T. Hemler, U. S. Navy, and Calvin Y. Sing at Massachusetts Institute of Technology's Gas Turbine Laboratory, Cambridge, Massachusetts.

Thesis Supervisor: E. S. Taylor
Title: Professor of Aircraft Engines

Table of Contents

List of Figures

INVESTIGATION OF ROTATING STALL IN A CENTRIFUGAL VANED DIFFUSER

DEFINITIONS USED IN THIS THESIS:

ROTATING STALL -- Intermittent partial or complete stalling of one or more blade passages of a compressor wherein the stalled portion rotates around the wheel in a tangential direction and the flow far upstream and far downstream of the wheel is unaffected.

STALL-FLUTTER -- Self-excited vibration of blades together with stall, such that there is coupling or feedback from flutter to stalling and unstalling, and from stalling and unstalling to flutter.

SURGE -- An audible pulsation of compressor pressure rise and weight-flow rate, wherein the flow far downstream and far upstream of the wheel has the same periodic pulsations of flow as are heard at the compressor.

I. INTRODUCTION

Recent investigations have shown that malfunctioning and structural failure of compressors, formerly attributed to stall-flutter and surge, have indeed been caused by rotating stall.

Stall-flutter has been investigated by Sisto, Ref. 1 and Schnittger, Ref. 2. More recently, Emmons in Ref. 3 has investigated compressor surge and stall phenomena. Huppert and Benser in Ref. 4 show the results of studying rotating stall in an axial compressor.

The more recent investigations have shown that some compressor acceleration difficulties are attributable to rotating stall. Even more important, blade failures and complete structural failures have resulted from rotating stall.

It is imperative, therefore, to know when, where, and under what conditions rotating stall will occur.

Present knowledge of rotating stall consists of:

(1) Its definition.

(2) Observed tests in cascades and axial compressors -- both single and multi-staged.

(3) The not disproven theory that rotating stall is due to inertia effects of air flow in the passages and a time lag from

blade stall until the upstream fluid feels the effect of that stall.

There is a dearth of material regarding rotating stall in centrifugal machines, although the British report one instance of it in Ref. 5. In an effort to accumulate evidence for more analytical studies, the flow through a centrifugal vaned diffuser was observed in this study. Conditions of angle-of-attack, mass flow, pressure in the passages, velocity, solidity factor and blade types were varied during this investigation.

The broad purposes of this thesis are two-fold:

(1) To verify or nullify present theory as to the nature of rotating stall by the study of centrifugal flow and subsequent comparison with axial flow and cascade data.

(2) To prepare the groundwork for future analytical or laboratory studies of the phenomena, and to indicate the desired direction for these future investigations, by accumulation of data concerning rotating stall.

This investigation was accomplished by two postgraduate students at M.I.T.: Lt. Frank T. Hemler, U. S. Navy,

attached to the U.S. Naval Postgraduate School program, and Calvin Y. Sing, both of whom were working towards their Science Master degree in Aeronautical Engineering. The investigations were accomplished in the Gas Turbine Laboratory of M.I.T. during the period of September 1953 through May 1954.

Thanks is expressed here to the thoughtful supervision, guidance, and suggestions made by Prof. E. S. Taylor of M.I.T.'s Gas Turbine Laboratory. Many other individuals in the Gas Turbine Laboratory and M.I.T. helped the authors tremendously.

II. EQUIPMENT

The Centrifugal Vaned Diffuser

The major component used in these tests was a centrifugal vaned diffuser. This type of diffuser was studied rather than a cascade in order to allow the flow to reenter upon itself. Further, a cascade study would not maintain the desired conditions long enough for full investigation. The exterior of the setup as used in M.I.T.'s Gas Turbine Laboratory is shown in Figs. 1 and 2.

Construction details of the centrifugal diffuser used can be found in Appendix A. As can be seen in Appendix A and Fig. 1, it is possible to vary the angle of flow.

The angle of flow as used in this report is that angle measured between the flow and a tangent to the inlet circle of the diffuser section. Rotation of the nozzle blades varies the departing flow angle from ten degrees to twenty degrees, as shown in Fig. 3. This variation allows different angles of attack for the stationary test blades.

The test blades are permanently in place when once inserted in the blade ring. Appendix A and Figs. 4 and 5, show that the entire blade ring with blades installed can be removed from the test rig. Figs. 6, 7, and 8 show the blades that were

used in the experiments covered by this report. The blades themselves are discussed later in this section. The blades shown in Fig. 6 were milled out of a solid aluminum ring. They are integral with the blade ring. The blades shown in Figs. 7 and 8 were machined individually. After making the blade forms, two holes were drilled in the sides. Pins of #29 drill rod were inserted into these holes with a press fit. This left the blades with two pins projecting from the sides, as shown in Figs. 7 and 8.

Another blade ring was made out of steel. Holes were drilled into the steel blade ring to match the projecting pins of the blades. In this manner, the blades could be inserted and removed at will, but a press fit insured against accidental removal. Also, as the test section is brought up flush with the cover plate as described in Appendix A, no flutter of the blades is possible. The cover plate and test section (blades) are held together by the force of the thrust nut.

The angle of attack of the blades shown in Fig. 7 and the angle of incidence of the blades shown in Fig. 8, was 14.1 and 15 degrees, respectively. These angles were incorporated in the blade ring. The flow angle and the angle of attack (or angle of incidence) were additive as shown in Appendix B.

Three different sets of blades were used. The first set used was the one shown in Fig. 6. Shape details of this set of blades can be found in Fig. 9. These blades are used in the General Electric C-14 diffuser. The second set of blades were blades of the form NACA 65-(12) 10 transformed from rectangular cascade form to a circular diffuser cascade. Fig. 7 shows the transformed blades. Appendix B shows how the rectangular cascade was transformed into the circular diffuser by means of conformal transformation. Ref. 6 gives a development of the method and equations used in this conformal transformation. The third set of blades were flat plates as shown in Fig. 8. These flat plates were milled with all edges sharp.

The Gas Turbine Laboratory and Facilities

The Gas Turbine Laboratory is an integral part of M.I.T., situated on its campus in Cambridge, Massachusetts. One part of this laboratory's equipment is a De Laval Air Compressor made by the De Laval Steam Turbine Co., Trenton, N.J. This compressor is run by a General Electric d.c. motor. The compressor is rated at 15,500 cuft per minute discharge, 5.33 psia suction pressure, 16.0 psia discharge pressure, 700 brake horsepower, at a compressor speed of 4060 RPM. Fig. 10 is a line diagram of the test set-up, showing necessary valves, gauges

and piping. Lines to and from other equipment serve such things as a small supersonic tunnel, etc. These other pieces of equipment were isolated for any run. Gauges and lines necessary to run the compressor, but unimportant to the experimenter are not shown in Fig. 10. Gauges shown are total temperature and total pressure gauges. Lines to and from the test diffuser are eight inch pipes.

Instrumentation and Reading of the Test Set-up

From the readings of RPM, pressures, and temperatures, it was possible to compute the operating point on the compressor map shown in Fig. 11. Fig. 11 also shows how to compute the factors necessary to establish that point. The mass flow and the velocity at any point in the test set-up could be computed.

It was necessary to: (1) distinguish between surge and rotating stall, (2) establish the speed of rotation, if rotating stall occurred, (3) establish the size of the rotating stalled region and (4) establish the number of stalled regions around the diffuser perimeter. It was also desirable to look at the flow in the channels in order to obtain some idea of what was happening and where.

The authors decided to meet the first three problems by using barium titanate crystals spaced at angles of 0, 72.5, and 180 degrees. These angles were chosen to give positive

identification of the stalled regions. Radially, the crystals were placed at 8.5 inches. This distance put the crystals in blade passages near the upstream end of those passages. It also enabled the crystals, which are one-half inch in diameter, to be placed so that no blade touched the crystals.

Some tests made on the crystals by the authors are included in Appendix C. These test results showed the suitability of the crystals for these experiments. The crystals were pressed into brass plugs of three-quarter inch outside diameter, which, in turn, were centered at the positions already indicated. Shielded leads went from the crystals to a RCA Cathode Ray Oscilloscope No. 160-B. The leads were run in parallel. The leads from the crystal at the 72.5 degree position were reversed in polarity for further identification. Of the first three problems previously outlined, the set-up as stated eliminated these problems as follows:

(1) Rotating stall would appear as shown in Fig. 12a, while surge would appear as in Fig. 12b. In other words, surge would occur at even intervals, while rotating stall would be at uneven intervals, due to the arrangement of the crystals.

(2) Regarding the speed of the stalled re-

gion -- should rotating stall be encountered, it would be only necessary to impose a known frequency on the oscilloscope, and measure the ratio between the known and unknown. Then, knowing the geometry, the speed could be determined.

(3) The size of the stalled region can be measured from the elapsed time for the stalled region to pass one crystal. The time would be measured by comparison with a known frequency.

In order to solve problem (4) and to observe the flow, a 2 1/2 inch diameter observation plate was made of plexiglass. This plate was pierced eccentrically with a wife which held many strings to be used as tufts. The observation plate is shown in Fig. 13. A matching hole was drilled in the front cover plate into which the observation plate fitted. Fig. 1 shows the observation plate in place, held by a shoulder of the plate and two brackets. The eccentricity of the tufts allowed them to be rotated, while the blades and back plate could be loosened and rotated. These two variables allowed the whole field of the vaneless diffuser to be

observed. Problem (4) was solved for slow speed rotation by observing the tufts and for high speed rotation by angularity relations of the crystals and a known frequency.

III. PROCEDURE

During the course of these investigations, the crystals were polarized twice as described in Appendix C. This was done to keep the crystals accurate and reliable. Six crystals were polarized and three crystals were selected by testing on the oscilloscope for equal deflections from a constant tone. The selected crystals were placed in the brass plugs, and mounted in the front plate. An ohmmeter was then used on each of the leads to ascertain that there were no shorts and no leads were grounded. The leads were hooked to the oscilloscope as shown in Fig. 1 and again checked with an ohmmeter.

The test rig was assembled as shown in Appendix A. The tufts were inserted as shown in Fig. 1. A final check with the ohmmeter on the crystal leads was then made. Prior to each run the local temperature and barometric pressure were recorded.

During Each Run

After opening the outlet and inlet valves of the test rig, the laboratory mechanic brought the De Laval air compressor

up to the desired operating point. This desired operating point was obtained as follows:

(1) The compressor was brought to an RPM thought to be correct.

(2) Closing of the atmospheric inlet valve isolated the system.

(3) Readings of P_{01}, P_{02}, T_{01}, and RPM were taken.

(4) As shown in Appendix D, the actual operating point on the compressor map was then calculated.

(5) From the actual operating point, adjustments were made to the RPM and by-pass valve until the desired operating point was obtained. This was done by trial and error, calculating each intermediate operating point as steady-state conditions were attained.

This desired point was chosen from the compressor characteristic map. The flow angle desired was set at the test rig.

The above conditions were held while the oscilloscope was surveyed from five to five thousand cycles. Then the passages

were surveyed with the tufts in the observation plate.

Maintaining the same operating point on the compressor map, a different flow angle was selected. Again, survey of the oscilloscope ranges and a survey at the blade passages with the tufts were made. The same procedure was carried out until all the desired flow angles were checked. At this point, another operating point on the compressor map was chosen. The same procedure outlined above was carried out for the new operating point. The above procedure was repeated until all the desired operating points were checked with each set of blades.

In order to check on the solidity factor, the runs made with 36 of the NACA blades were repeated with every other blade removed.

After each run, when the compressor was shut down, the crystal leads were checked with the ohmmeter for continuity. Each crystal was individually checked to make certain it was still operating correctly.

The order of blades used was:

(1) C-14 blades -- Fig. 6

(2) NACA blades -- Fig. 7

(3) Flat plates -- Fig. 8

Generally speaking, for each set of blades, the

same points on the compressor map were investigated. Table I lists the operating points used. Slight variations from these points occurred for two reasons:

(1) As the nozzle blades were opened or closed, the mass flow was altered slightly. This altered the pressure ratio and mass flow factor. Checking on the operating points when the nozzle blades went from full opened to full closed altered the operating point so little that the change could not be plotted.

(2) It was very hard to obtain the exact same point in two different runs with the air compressor. Arbitrarily, it was decided that a variation of 0.025 in the mass flow factor and 0.05 in the pressure ratio, on the compressor map, would be considered the same point.

For each operating point, the flow angles set were 10, 15, and 20 degrees.

Three "auxiliary" runs were made. One run consisted of finding what occurred when a blade was set over one of

the crystals. The blades were placed over the crystals and the oscilloscope patterns were compared with the previous patterns when the crystals were in the passage. The second "auxiliary" run consisted of investigating the diffuser when the air compressor was surging. This operating point is point number nine of Table I. The third "auxiliary" run was made from operating point number 4, with the NACA blades. After the routine surveys, the exhaust valve from the test rig was closed down until the main air compressor surged. A survey was then made with the tufts and oscilloscope.

The original procedural plan of the authors' was to accomplish what is outlined above, until rotating stall was encountered. As soon as rotating stall was encountered further testing would be in the region of the rotating stall. This investigation would include pictures of the oscilloscope, patterns and tape recordings of any unusual sounds, in addition to that outlined above.

IV. RESULTS AND DISCUSSION

Table I shows the nine operating points that were used. Placing these points on the compressor map, Fig. 11, shows that the points were chosen for the following reasons:

(1) Points 1, 2, 3, 4, 6, and 7 are just inside the surge line. This gave the maximum usable pressure ratio range from the air compressor.

(2) Points 5 and 8 were chosen to see if there were any peculiarity of upstream flow. The oscilloscope patterns and tufts would then indicate unusual conditions or possibly rotating stall. In picking the points 5 and 8, it was appreciated that only the pressure ratio should effect the test set-up. This is because the guide vanes choked with high mass flow. This necessitated opening the by-pass valve shown in Fig. 10 in order to attain points 5 and 8. In effect, the compressor operated at points 5 and 8, but the test section operated at the same pressure

and a lower mass flow.

(3) Point 9 was chosen to investigate conditions during mild surge of the compressor.

Appendix D shows the calculations necessary to determine an operating point.

THERE WAS NO INDICATION OF ROTATING STALL AT ANY OF THE CONDITIONS INVESTIGATED.

Stall-flutter was effectively eliminated by the press fit of the blades into the blade rings on one edge, and by the force of the cover plate on the other edge. This system held the blades firmly along both edges, as shown in Appendix A.

Oscilloscope indications consisted mainly of random noise. At approximately 4,200 cycles a wave of sinusoidal form was noted. This wave form was present at every condition investigated. It was not the RPM of the compressor, since this varied. This sine wave was probably caused by a whistle in the piping. Because of the sinusoidal form, it was concluded that this wave had no bearing on surge or rotating stall.

Occasionally higher amplitude blips were noted. These were infrequent and had no recurrent pattern.

As shown in Sketch 1, the C-14 blades gave tuft indications of stalled and unstalled blades as the angle of flow was

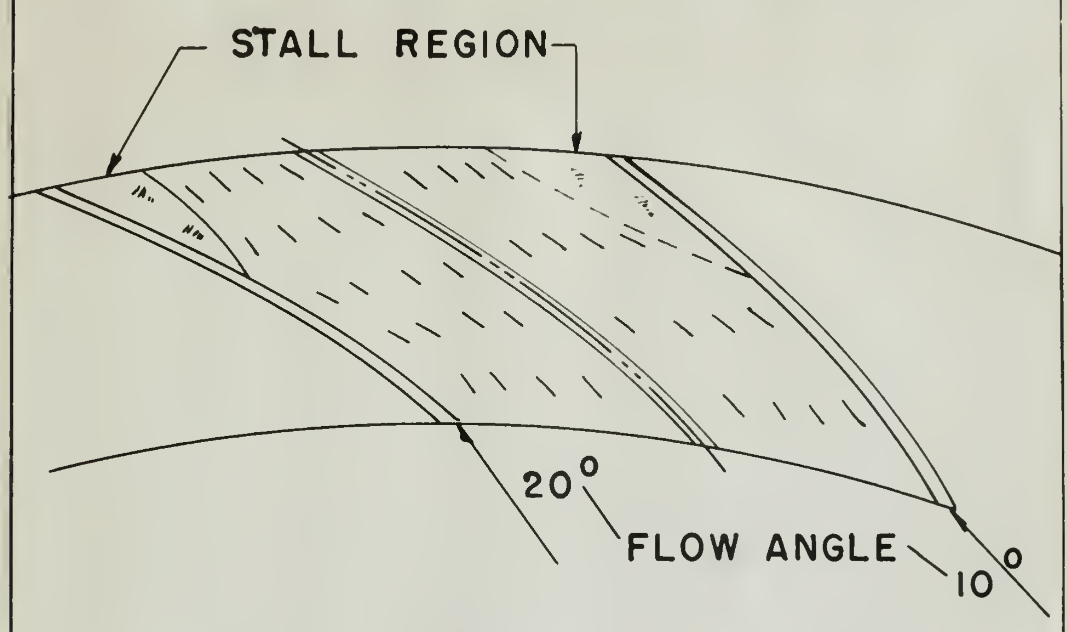

TUFT INDICATIONS - C14 BLADES

SKETCH I

varied from 10 to 20 degrees, respectively. The flow angle was shifted very slowly so that all blades went from the unstalled to the stalled condition. Nothing unusual occurred. The transition was quick and positive, regardless of how slowly the angle of flow was altered. While the blades were unstalled, but close to the stalling flow angle (approximately fifteen degrees), a brass rod was inserted into the downstream flow of the nozzle blades. It was hoped that the wake effect would stall one or more passages and that rotating stall would occur. It didn't.

During the tests with the NACA 65-(12) 10 blades, the separation point remained very close to 1 1/2 inch from the trailing edge. It moved forward slightly at a flow angle of 10 degrees, but no more than 1/4 of an inch. It moved back a like amount at 20 degrees flow angle. This movement decreased to an imperceptible amount at low mass flows.

The blade passages were never completely turbulent with the NACA 65-(12) 10 blades installed.

When the solidity factor was varied by reducing the number of blades from 36 to 18, there was no change in any of the foregoing results.

With the flat plate installation, (even with 18 plates), the passages were turbulent all the time. This is attributable to the following sequence of facts:

(1) The sharp leading edges made the separation point occur near the leading edge.

(2) The flow angle was effectively 10 to 20 degrees.

(3) (1) and (2) put each succeeding blade in the stalled region of the blade ahead of it.

(4) Each blade and passage then became

fully turbulent.

With the flat plates installed, at low mass flow, the tufts indicated turbulent flow on the pressure side of the blade, as shown in Sketch 2.

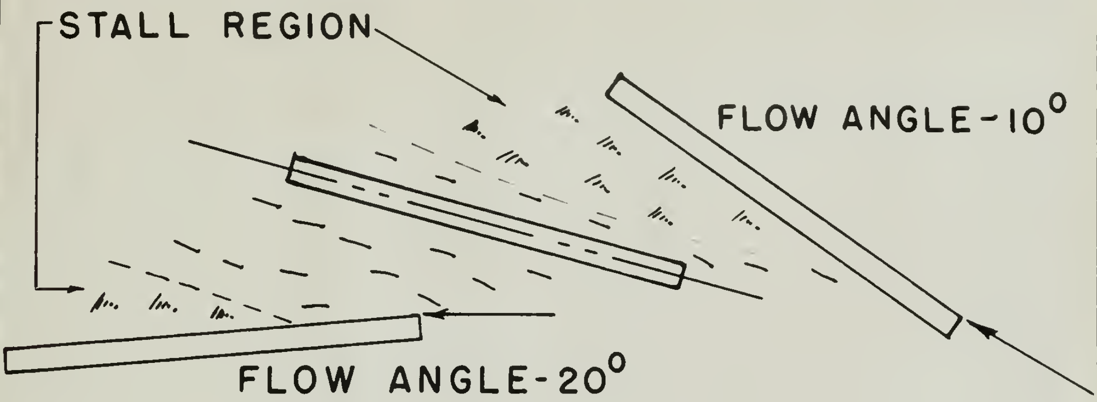

TUFT INDICATIONS-FLAT PLATES

SKETCH 2

This occurred at a flow angle of ten degrees. This phenomenon occurred only once and could not be repeated. No explanation is offered for its occurrence.

The C-14 blades were picked for these experiments for two major reasons. First, they are in use commercially.

Secondly, they were available at the beginning of these tests, which meant that the test set-up could be checked quickly as to its adequacy for this investigation. In addition, results of C-14 blade runs would give some clue as to the trend of experiments to be followed in the future.

Upon completion of the investigation of the C-14 blades, it was decided to try a NACA 65-(12) 10 blade. This blade reputedly had a gentle C_L-α curve near the stall point, as shown in Fig. 14a. This decision involved the present theory of rotating stall as explained in Refs. 3 and 4. For clarification, a quick review of that theory is presented here.

A rectangular cascade is formed as shown in Fig. 15. Assume an angle of attack, as shown, which is just below stalling; i.e., any increase in angle of attack will cause stalling. Further assume some small perturbation causes a transitory increase in the angle of attack of blade number 2. This causes blade 2 to stall. This stalling causes more low energy air in the passage. The high energy air now has less area to pass through. This partial blocking of passage B causes upstream air to be diverted to blade passages A and C. There is a time lag from the time the blade stalls until the upstream air feels this stall. The diversion of upstream air causes the angle of attack on blade number 3 to

Secondly, they were available at the beginning of these tests, which meant that the test set-up could be checked quickly as to its adequacy for this investigation. In addition, results of C-14 blade runs would give some clue as to the trend of experiments to be followed in the future.

Upon completion of the investigation of the C-14 blades, it was decided to try a NACA 65-(12) 10 blade. This blade reputedly had a gentle C_L-α curve near the stall point, as shown in Fig. 14a. This decision involved the present theory of rotating stall as explained in Refs. 3 and 4. For clarification, a quick review of that theory is presented here.

A rectangular cascade is formed as shown in Fig. 15. Assume an angle of attack, as shown, which is just below stalling; i.e., any increase in angle of attack will cause stalling. Further assume some small perturbation causes a transitory increase in the angle of attack of blade number 2. This causes blade 2 to stall. This stalling causes more low energy air in the passage. The high energy air now has less area to pass through. This partial blocking of passage B causes upstream air to be diverted to blade passages A and C. There is a time lag from the time the blade stalls until the upstream air feels this stall. The diversion of upstream air causes the angle of attack on blade number 3 to

increase and on blade number 1 to decrease. This in turn will cause blade 3 to stall, while blade 1 is further away from the stall point. As passage C now diverts air to passages B and D, blade 2 tends to unstall and blade 4 to stall. Therefore, this stall can be seen to be progressing upward.

With rotating compressors, the motion of the wheel in Fig. 15 would be down. Recent experiments have shown the speed of rotating stall to be about 1/2 the wheel speed in the direction of rotation. The vectors of Fig. 15 represent this condition.

Going back to the gentle C_L-α curve of the NACA blades, it was reasoned that the best chance of floating back and forth between stalling and unstalling would occur when very small changes in lift produced a substantial change in the angle of attack. In other words, a small change in energy produced comparatively big changes in angle of attack. Data published by the NACA is readily available on many airfoils. Of these airfoils, the NACA 65-(12) 10 has a very gentle C_L-α curve.

Since the results of the NACA blades showed no rotating stall, it was decided to go to the opposite extreme. Consequently, flat plates were the next forms tried. These flat plates have a C_L-α curve something like Fig. 14b. Although separation occurred at the leading edge on the flat plates and the

whole passage was turbulent, no rotating stall was found.

Why was no rotating stall found at any time?

The present theory of rotating stall mentions inertia and time lag. Since these two phenomena are both inherent and unavoidable, they were present in this test section. The flat plates were stalled with the flow in the passages turbulent at every operating condition. The NACA blades did stall, but the flow in the passages was mostly laminar. The C-14 blades reacted in both of these ways, but under different conditions. With a flow angle of ten degrees, the C-14 blades were stalled and the passages turbulent. With a flow angle of twenty degrees, the C-14 blades were stalled with a negative angle of attack. Any condition, in between these extremes could be obtained by varying the flow angle. Laminar flow could be obtained between the extremes. Attempts to instigate a rotating stall were made by changing the mass flow, velocity, pressure, blade form, solidity factor, separation point and wake effects.

Could the failure to find rotating stall be caused by poor instrumentation? The crystals were checked before and after each major run; at no time was there any trouble with them. No shorts. No grounds. No broken leads. The crystals picked up a constant tone after the runs as well as before. With no

external amplifier, an approximate sine wave and random noise were obtained. With the same gain, the deflection produced by the random noise was greater than the deflection produced by a human being holding the leads. The deflections caused by the human being were 60 cycles, although he was not in immediate contact with any source of power.

Concerning the run, described in the Procedure, which was made with the blades placed upon the crystals, there was no noticeable change in the oscilloscope patterns. If anything occurred, it was merely a rounding of the highest deflections. When a blade was centered directly over a crystal, the crystal was still partially in the passage. It was concluded that partial covering of the crystals had negligible results on the oscilloscope patterns.

When the exhaust valve was closed slowly, the only effect was to increase the compressor's pressure ratio until it surged. Nothing unusual occurred to the oscilloscope patterns or to the tufts.

The tufts gave every indication that was expected of them including the surge of the air compressor. (This surge was very low in frequency, approximately 1 1/2 cycles per second.)

Therefore, the authors don't believe it was

instrumentation.

If the foregoing is true -- and the authors sincerely believe it is -- then the answer must be sought elsewhere.

Analytically, there may be a lack or error in the theory. The authors don't believe there is anything wrong with the theory as far as it goes, but there is more to the theory than has been expounded. It has been suggested that the dynamics of rotation must enter. This is disqualified quickly by the British in Ref. 5, wherein rotating stall was obtained in a stationary diffuser.

It appears that the phenomenon of rotating stall has the attributes of a self-excited but damped vibration of classical mechanics. The energy source is present in the air stream. By analogy, the air contains the damping force and the spring force. The authors think that the unstable region of a gentle C_L-α curve as shown in Fig. 14a would assist in starting rotating stall. A decrease in the effective damping force would occur since there would be little energy dissipated by the damping force until the stalled region had grown.

There must be some instability connected with rotating stall. Anything to increase that instability should aid in starting rotating stall.

It has been stated that the variables investigated by the authors were mass flow, velocity, pressure, solidity factor, angle of attack and blade form. These variables were not all altered individually; i.e., mass flow was varied, but other parameters such as velocity and pressure changed at the same time. This procedure was followed for two reasons:

(1) Time limitations prevented the altering of individual factors, if the entire field was to be surveyed.

(2) By accomplishing the outlined variations, it was hoped that the magic factor or combination of factors would be discovered. Then further investigation of this factor or group of factors could be undertaken.

The very method used suggests that the problem of rotating stall may be amenable to dimensional analysis. By Buckingham's method, the parameters used by the authors could be non-dimensionalized. (The blade form parameter should be enlarged to include length, thickness, C_L-α curves, and size and length of the passage between blades.) By experimentation, the unimportant non-dimensional factors could be eliminated.

Further experiments on important factors could then proceed more successfully.

Empirically, it is believed that there are two excellent channels open for further investigation:

(1) Make new guide vanes for this set-up. These new guide vanes are to increase the flow angle. Then by putting flat plates in the diffuser at the proper incidence angle, the leading edge of one plate would be out of the stalled region of the preceding plate. This study would show a better comparison between the two C_L-α curves, as discussed above.

(2) Last -- and most important! Set up the conditions encountered in Ref. 5, wherein a rotating stall was inadvertently produced and was not further investigated. Since this was a centrifugal diffuser, much valuable information should be obtainable from such a study, especially when compared with other present day experiments.

V. CONCLUSIONS AND RECOMMENDATIONS

No rotating stall was encountered at any of the conditions investigated. These conditions included varying pressure, mass flow, velocity, blade form, solidity factor and angle of attack. The failure to produce rotating stall lies not in the set-up, but rather in a lack of some factor in the present theory. The lacking factor is not the dynamics of rotation.

The lack may be that a larger unstable operating region of the effective C_L-α curve is needed. An analogy along this line can be made with self-excited vibrations in classical mechanics.

A strong recommendation is made by the authors to apply the methods of Buckingham's dimensional analysis to the problem of rotating stall.

Two experimental fields for further study should be:

(1) Increase the cascade flow angle when the flat plates are used. This will make the stalled region of one blade miss the leading edge of the adjacent blade.

(2) Reproduce and study the rotating stall produced in a stationary diffuser by the British in Ref. 5.

V. CONCLUSIONS AND RECOMMENDATIONS

No rotating stall was encountered at any of the conditions investigated. These conditions included varying pressure, mass flow, velocity, blade form, solidity factor and angle of attack. The failure to produce rotating stall lies not in the set-up, but rather in a lack of some factor in the present theory. The lacking factor is not the dynamics of rotation.

The lack may be that a larger unstable operating region of the effective $C_L-\alpha$ curve is needed. An analogy along this line can be made with self-excited vibrations in classical mechanics.

A strong recommendation is made by the authors to apply the methods of Buckingham's dimensional analysis to the problem of rotating stall.

Two experimental fields for further study would be:

(1) Increase the cascade flow angle when the flat plates are used. This will cause the stalled region of one blade enter the leading edge of the adjacent blade.

(2) Experiment and study the rotating stall produced in a stationary diffuser by the method in Ref. 5.

REFERENCES AND BIBLIOGRAPHY

1. "Stall-Flutter in Cascades", Sisto, F., Journal of the Aeronautical Sciences, September, 1953, Vol. 20, Number 9, pages 598-604.

2. "The Aerodynamic Mechanism of Vibrating Compressor Blades", Schnittger, Jan R., Sc. D. Thesis, Mech. Engrg. Dept., M.I.T., 1953.

3. "Compressor Surge and Stall Phenomena", Emmons, H. W., ASME Annual Meeting of November, 1953, paper number 53-A-65.

4. "Some Surge and Stall Phenomena in Axial Flow Compressors", Huppert, M. C., and Benser, W. A., Journal of the Aeronautical Sciences, December, 1953, Vol. 20, Number 12, pages 835-845.

5. The Institution of Mechanical Engineers Proceedings, 1945, Vol. 153, War Emergency Issue Number 12, page 438.

6. "Two-Dimensional, Incompressible Flow Study of Vaned Diffuser for Centrifugal Compressors", Faulders, C. R., Gas Turbine Laboratory, June 1953, M.I.T., Cambridge, Massachusetts.

7. "Experimental Investigations of Propagating Stall in Axial Flow Compressors", Iura, T., and Rannie, W. D., Mech. Engrg. Dept., Cal. Inst. Tech., ASME paper number 53-SA-69.

8. "Aerodynamic Interference Between Moving Blade Rows", Kemp, N. H., and Sears, W. R., Journal of the Aeronautical Sciences, September 1953, Vol. 20, Number 9, pages 585-597.

9. "Propagation of Stall in Compressor Blade Rows", Marble, F. E., Cal. Inst. Tech., paper presented at I. A. S. 21st Annual Meeting, New York City, January 1953.

Table I

DESIRED OPERATING POINTS

POINTS	$P_r = \frac{p_{o_2}}{p_{o_1}}$	π_{mi}	MFF
1	1.18	0.175	0.060
2	1.50	0.287	0.170
3	1.90	0.375	0.240
4	2.20	0.418	0.300
5	2.30	0.460	0.550
6	3.00	0.495	0.450
7	3.30	0.516	0.500
8	1.75	0.490	0.875
9	2.10	0.395	0.230

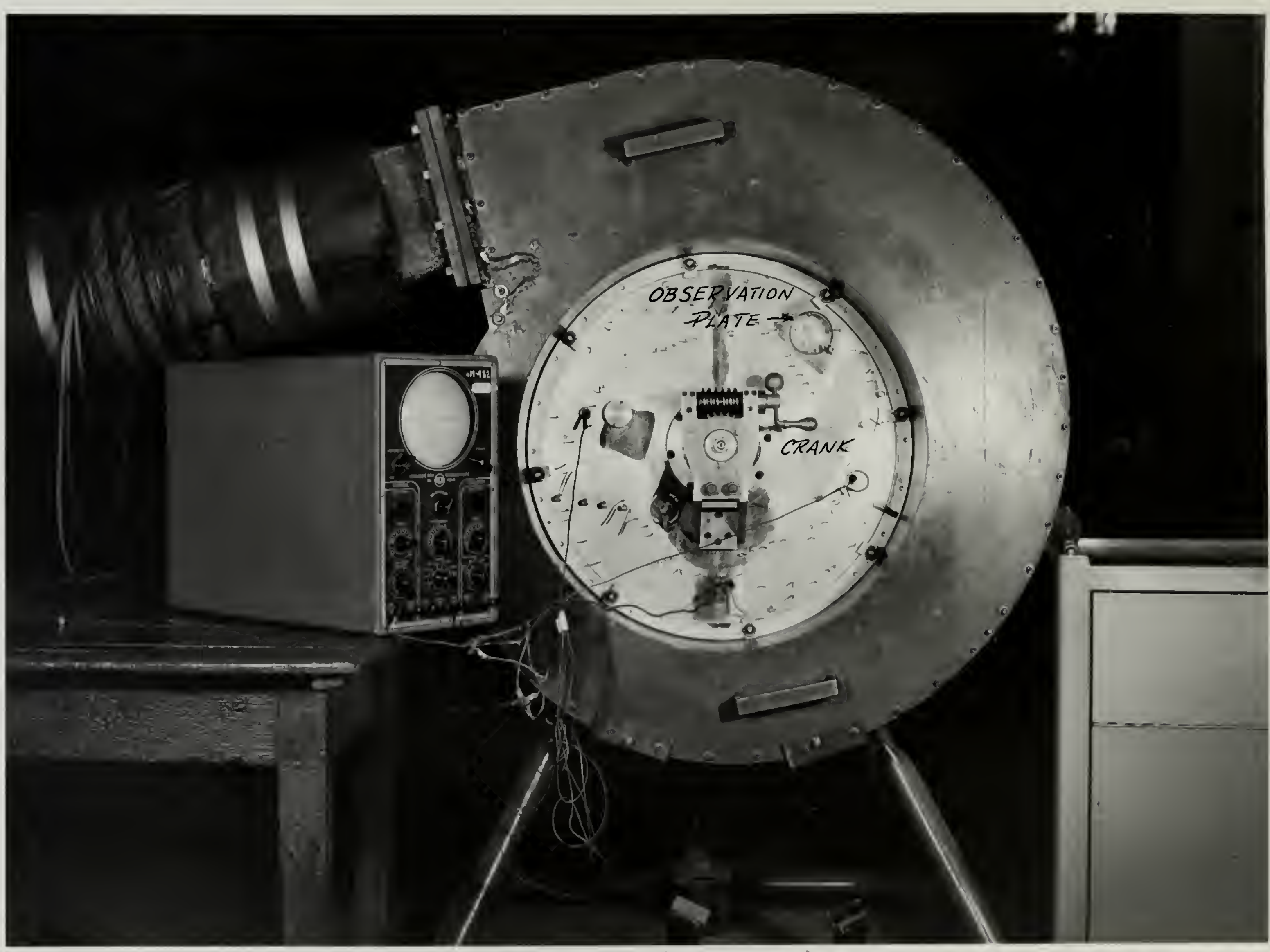

TEST SET-UP (FRONT VIEW)
FIG. 1

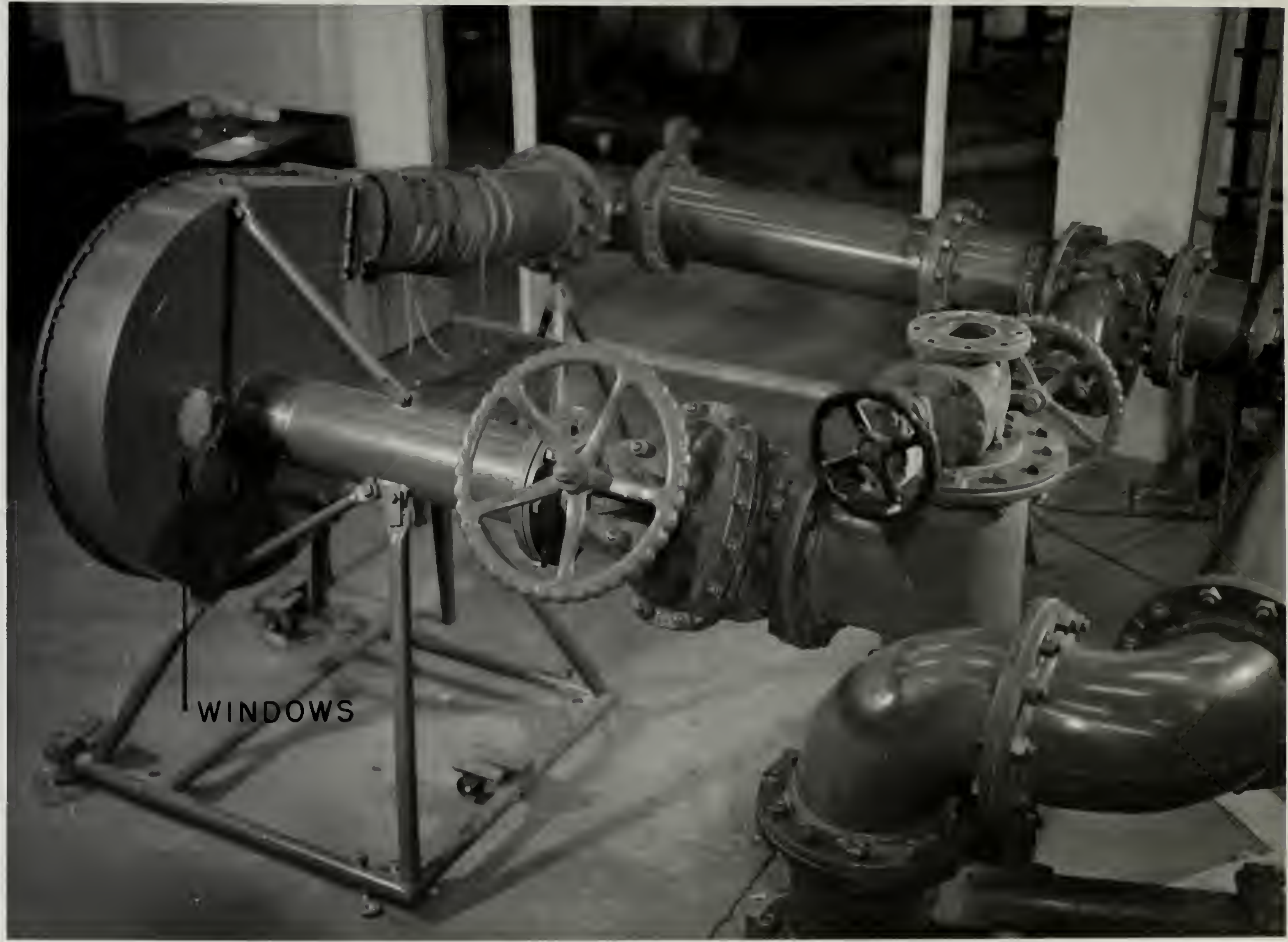

TEST SET-UP (SIDE VIEW)
FIG. 2

NOZZLE BLADES
FIG. 3

TEST SET-UP (OUTER COVER REMOVED)
FIG. 4

BLADE RING REMOVED
FIG. 5

C-14 BLADES
FIG. 6

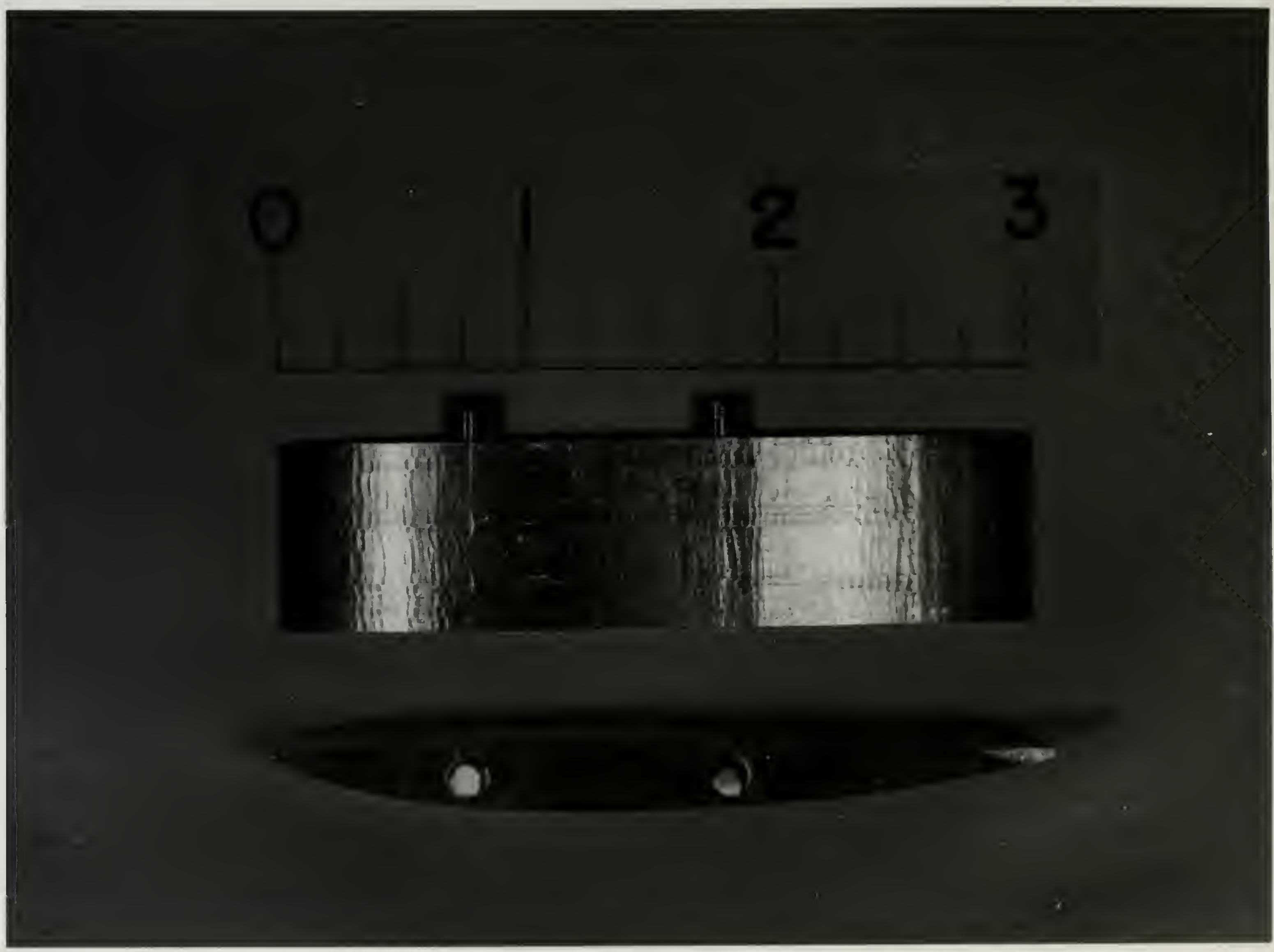

TRANSFORMED NACA 65-(12)10 BLADES
FIG. 7

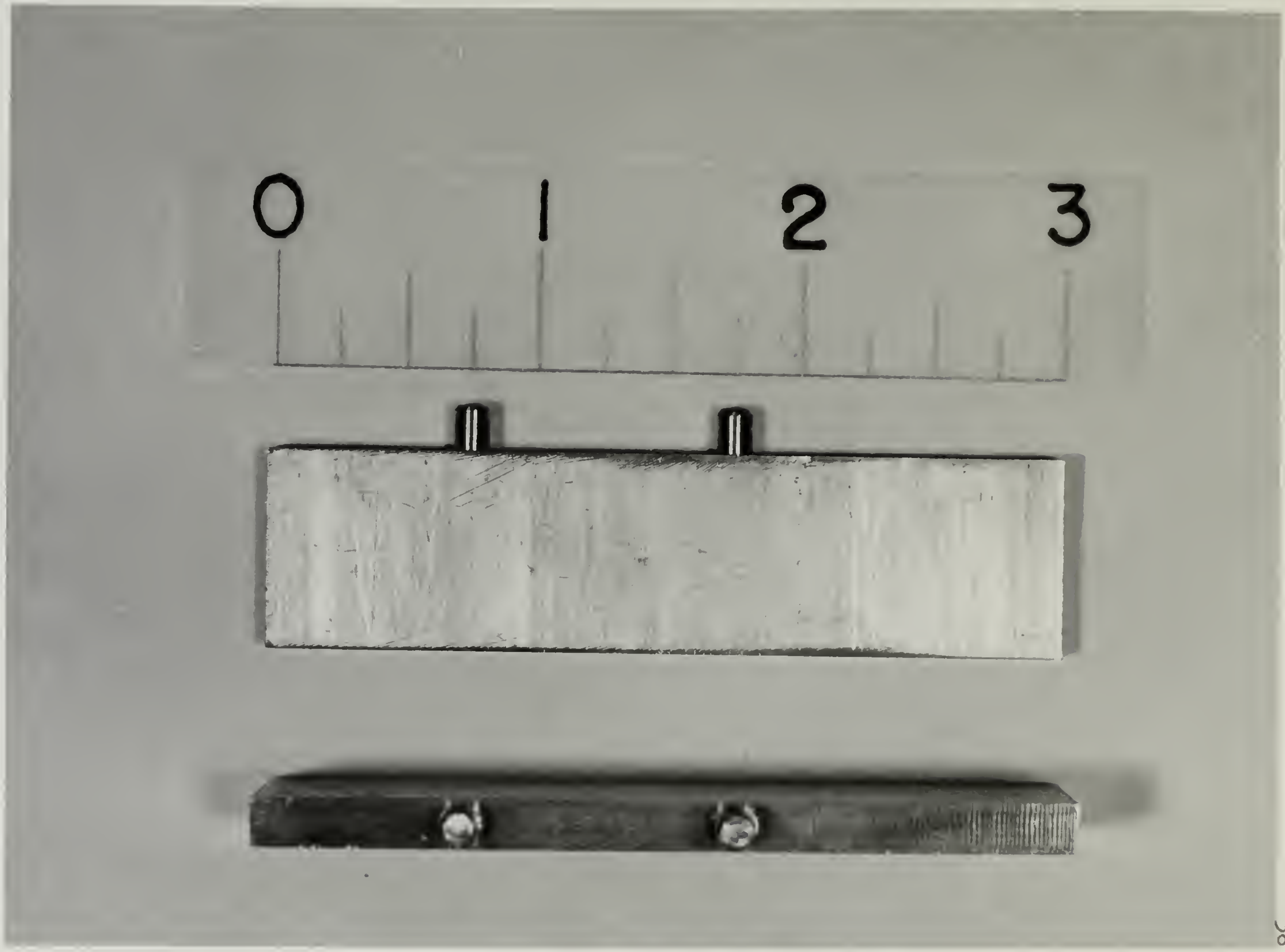

FLAT PLATES
FIG. 8

DETAILS OF THE C-14 DIFFUSER

BLADES

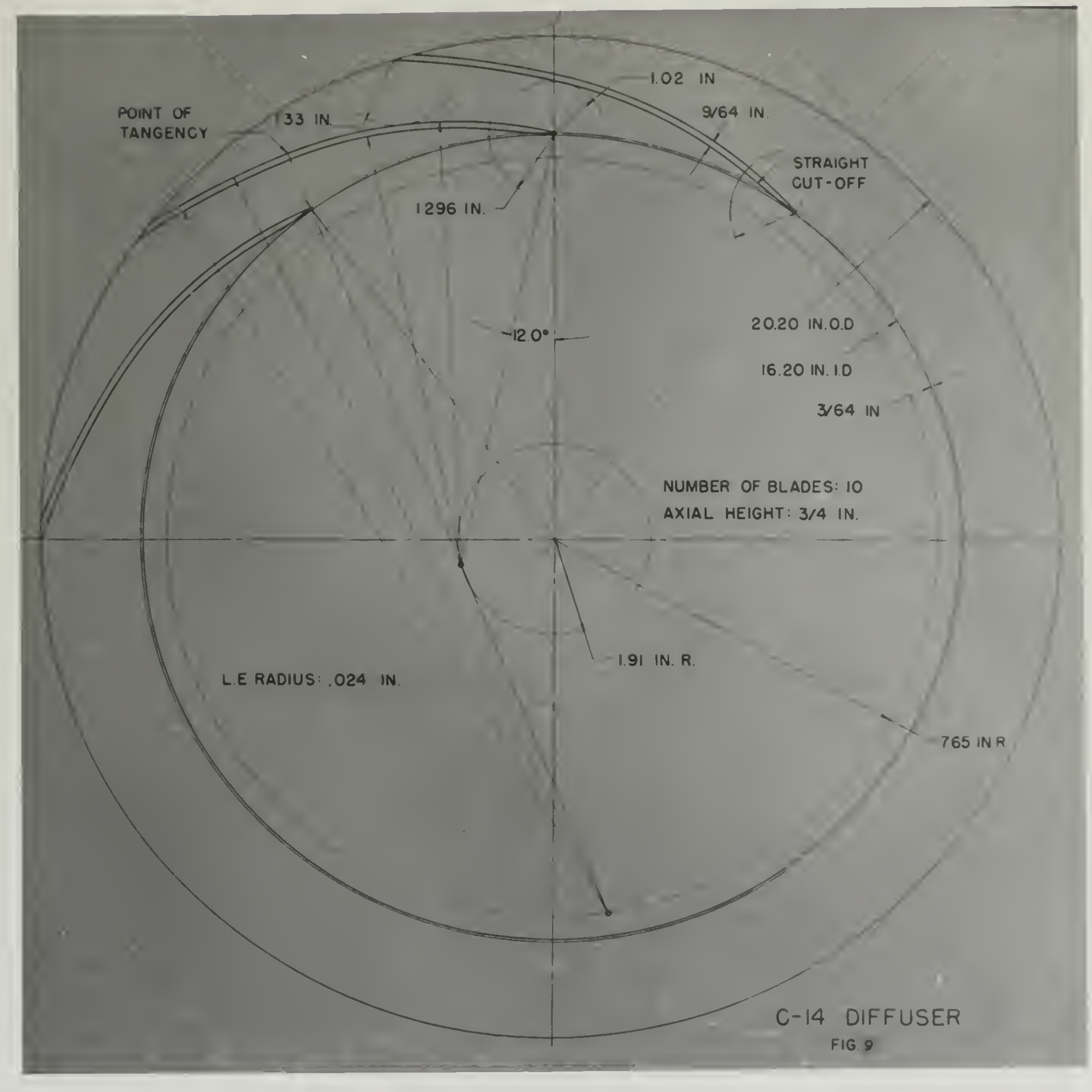

FIG. 9

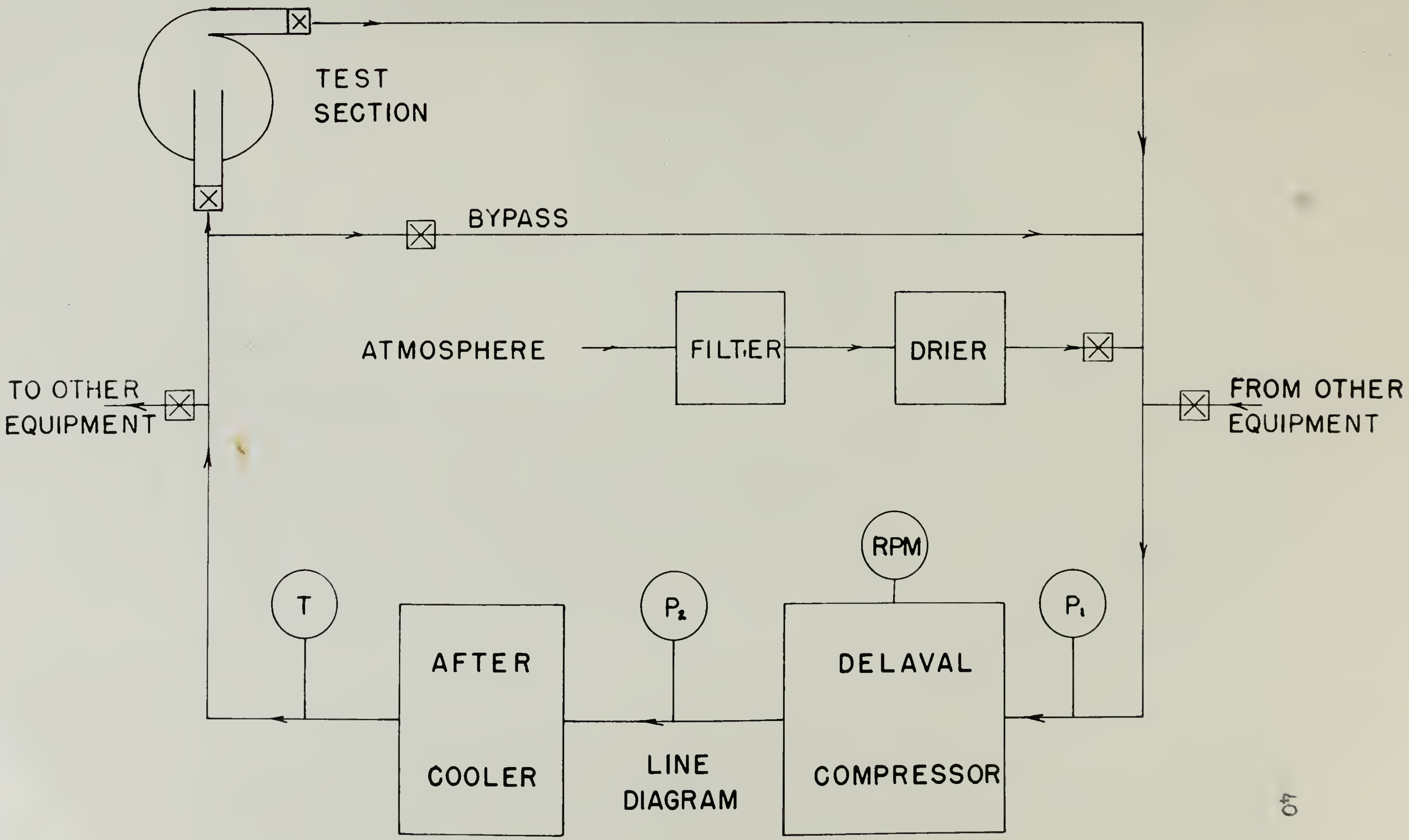
TEST
SECTION
BYPASS
ATMOSPHERE
FILTER
DRIER
TO OTHER
EQUIPMENT
FROM OTHER
EQUIPMENT
RPM
T
P2
P1
AFTER
COOLER
DELAVAL
COMPRESSOR
LINE
DIAGRAM

FIG. 10

MIT GAS TURBINE LABORATORY - WIND TUNNEL

DeLAVAL COMPRESSOR CHARACTERISTICS

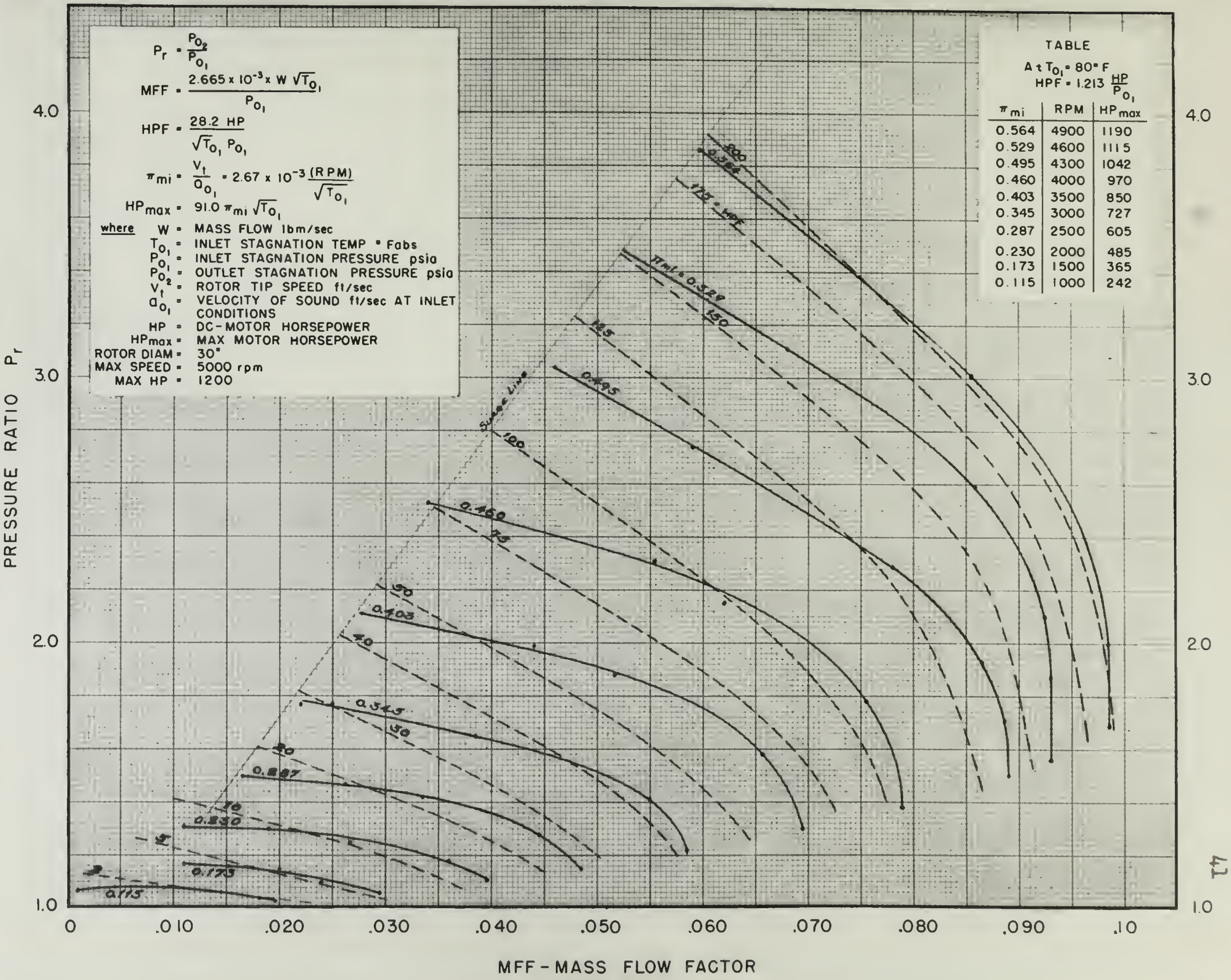

TABLE

A t T_{o_1} = 80° F

HPF = 1.213 $\frac{HP}{P_{o_1}}$

π_{mi}	RPM	HP_{max}
0.564	4900	1190
0.529	4600	1115
0.495	4300	1042
0.460	4000	970
0.403	3500	850
0.345	3000	727
0.287	2500	605
0.230	2000	485
0.173	1500	365
0.115	1000	242

FIG. 11

a
ROTATING STALL

b
SURGE

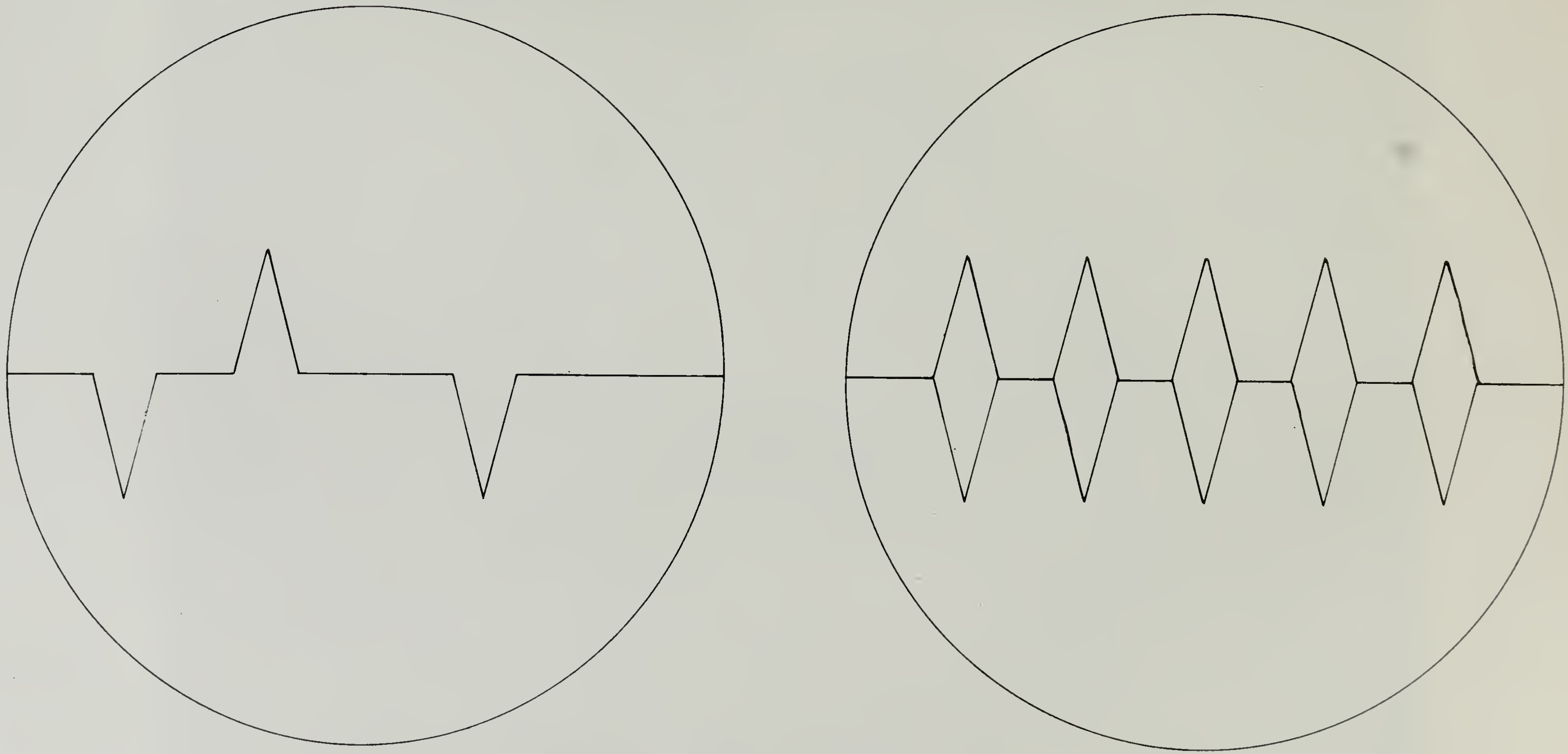

OSCILLOSCOPE PATTERNS

FIG. 12

OBSERVATION PLATE WITH TUFTS
FIG. 13

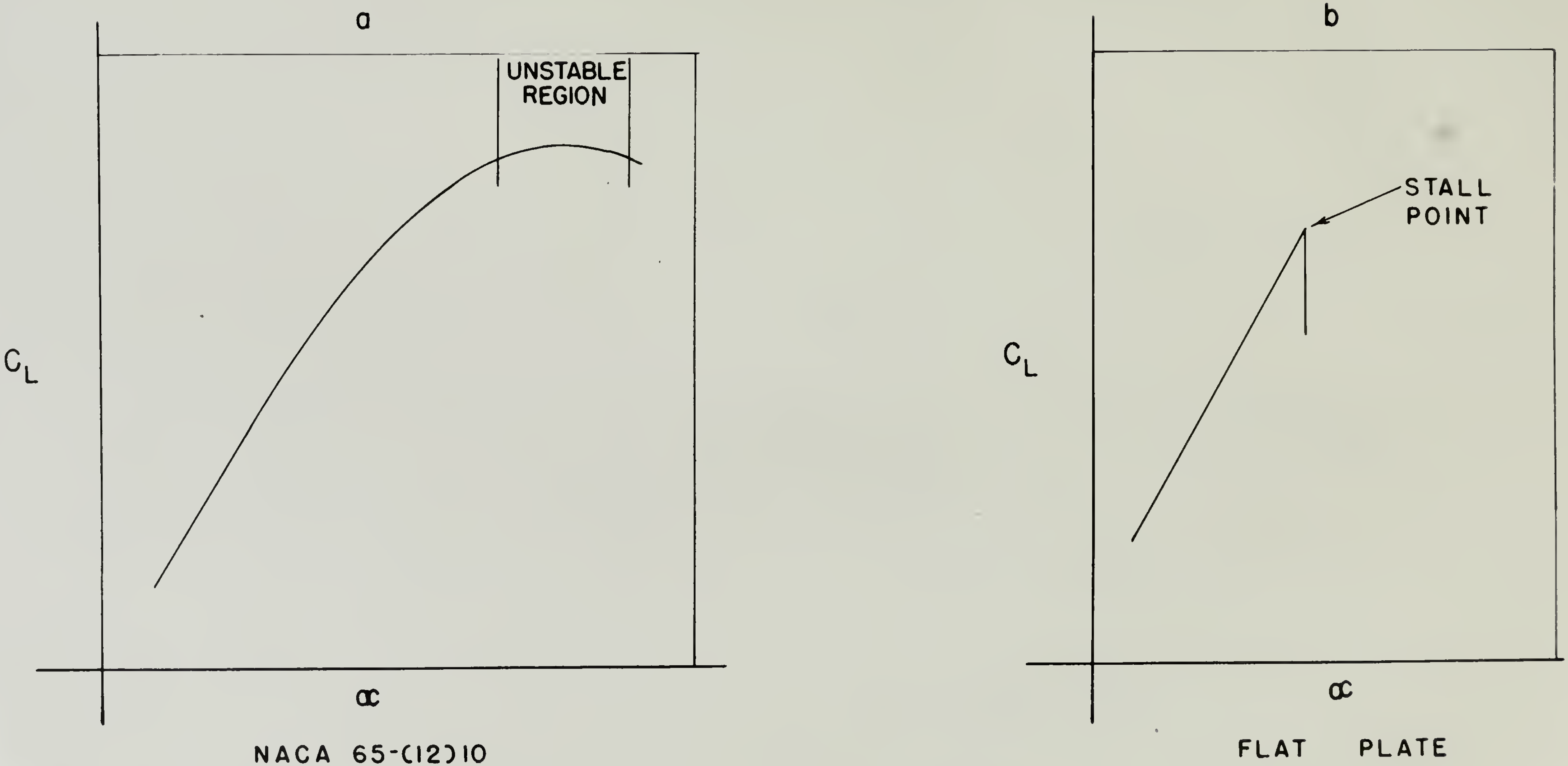

BLADE CHARACTERISTICS

FIG. 14

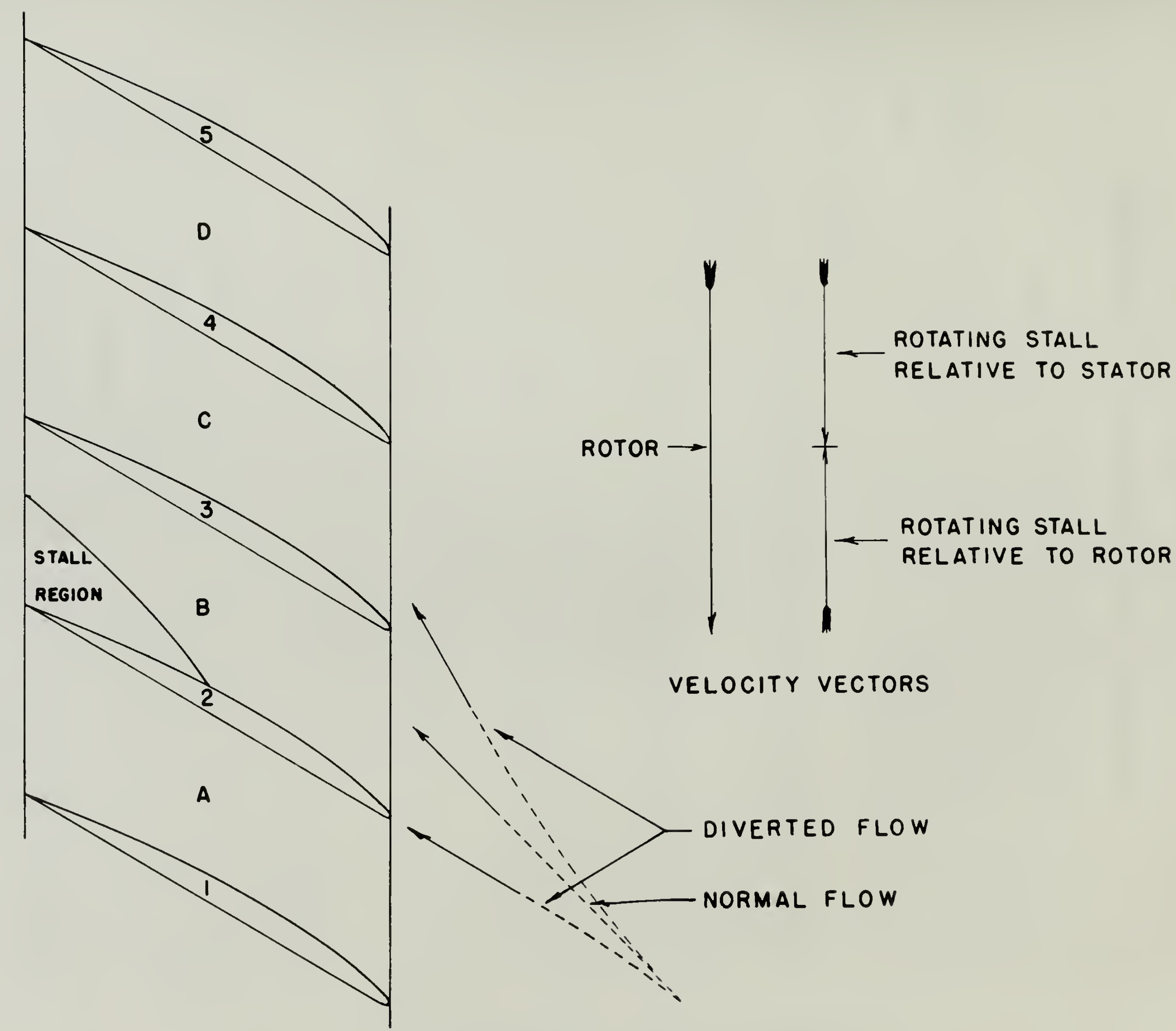

ROTATING STALL THEORY

FIG. 15

Appendix A

DETAILS OF THE DIFFUSER TEST SECTION

The diffuser test section is mounted in a collector manifold as shown in Fig. 1 of the thesis. It is supported by the cover plate and the inlet guide vanes as shown in Fig. A-1, of this Appendix.

To disassemble the test section the following steps are required:

(1) Remove the gearing mechanism as shown in Fig. A-1.

(2) Remove the hold-down lugs around the cover plate.

(3) Remove the cover plate.

(4) Remove the test section.

To remove the blade ring, turn the test section to a vertical position. Located on the back of the section are allenhead screws which hold the blade ring to the test section. After removing the screws, the blade ring can be forced out by inserting a drift into the screw holes. To assemble and remount the test section, the reverse of the above procedure is followed.

In order to rotate the test section the following procedure should be performed:

Appendix A

DETAILS OF THE DIFFUSER TEST SECTION

The diffuser test section is mounted in a collector manifold as shown in Fig. 1 of the thesis. It is supported by the cover plate and the inlet guide vanes as shown in Fig. A-1 of this Appendix.

To disassemble the test section the following steps are required:

(1) Remove the gearing mechanism as shown in Fig. A-1.

(2) Remove the hold-down lugs around the cover plate.

(3) Remove the cover plate.

(4) Remove the test section.

To remove the blade ring, turn the test section to a vertical position. Located on the back of the section are Allen-head screws which hold the blade ring to the test section. After removing the screws, the blade ring can be forced out by inserting a drill into the screw holes. To assemble and mount the test section, the reverse of the above procedure is followed.

In order to rotate the test section the following procedure should be performed:

(1) Turn the bronze thrust nut on the gearing mechanism clockwise to release the test section from the cover plate.

(2) Turn the crank, located on the gearing mechanism as shown in Fig. A-1. This will turn the test section to any desired position.

(3) To lock the test section in the desired position, turn the bronze thrust nut counter-clockwise until the test section is flush against the cover plate. This anchors the blades firmly, preventing flutter.

In order to change the angle of flow it is necessary to rotate the nozzle blades. This is accomplished as follows:

(1) Roughly align the nozzle blade angle indicating marks, located on the back of the test section, with the scribed line on the upper window of the two plexiglass windows. These windows are located on the back of the collector manifold, as shown in Fig. 2 of the thesis.

(2) Lock the nozzle blade turning ring. This

is done by turning the round-head screw, (located in one of the plexiglass mounting screw holes), into a hole that should be almost in line with the screw. The test section may have to be moved slightly to insert the screw properly.

(3) To rotate the nozzle blades turn the gearing mechanism located on the cover plate. By aligning the indicating marks the flow angle is determined. The middle position gives an angle of flow of 15 degrees, the upper position 20 degrees and the lower position 10 degrees.

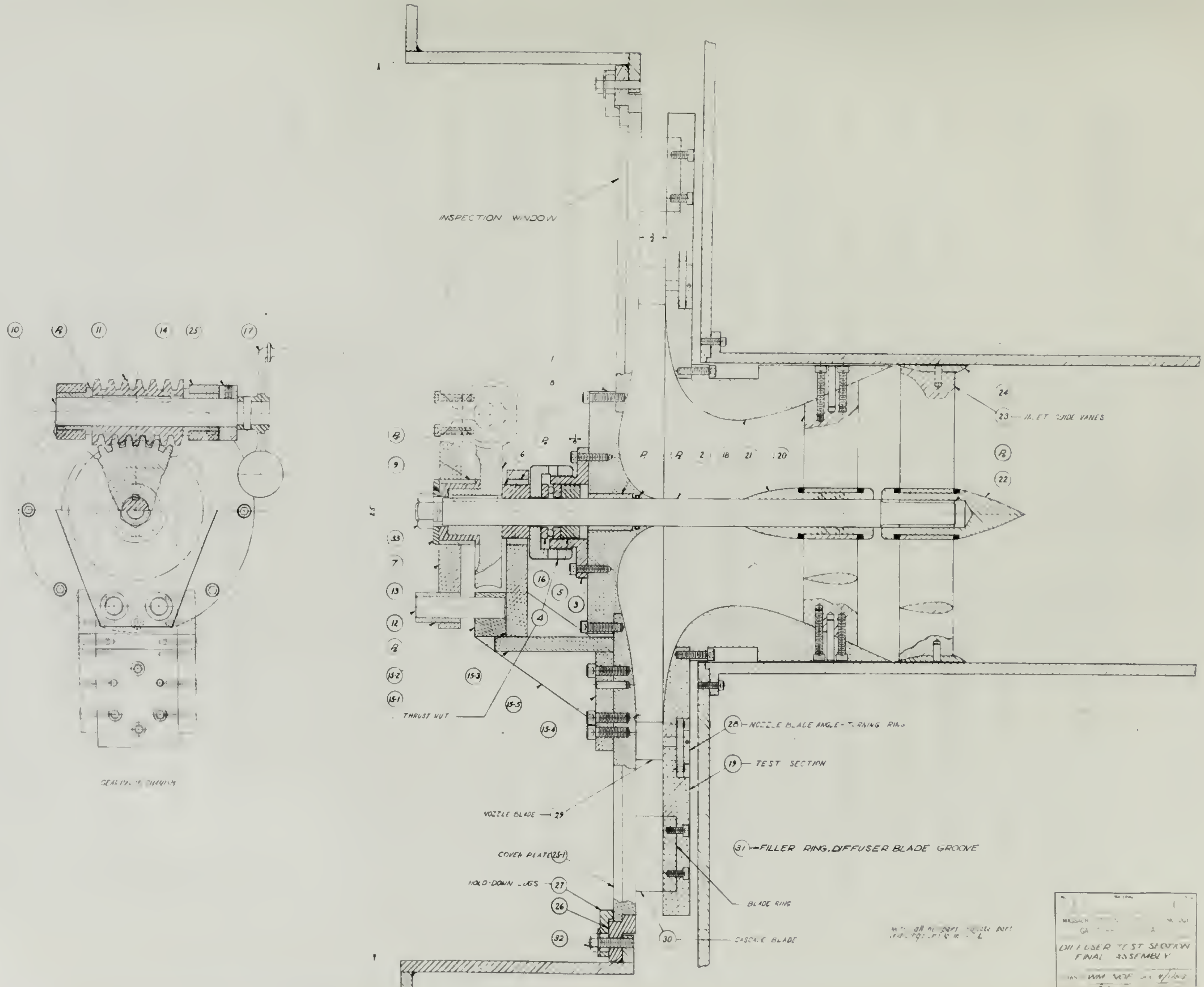
INSPECTION WINDOW
INLET GUIDE VANES
THRUST NUT
NOZZLE BLADE ANGLE-TURNING RING
TEST SECTION
NOZZLE BLADE — 29
FILLER RING, DIFFUSER BLADE GROOVE
COVER PLATE (25-1)
HOLD-DOWN LUGS
BLADE RING
CASCADE BLADE
DIFFUSER TEST SECTION
FINAL ASSEMBLY

FIG. A-1

Appendix B

CONFORMAL TRANSFORMATION OF NACA 65-(12)10 BLADES

Ref. 5 of the thesis gives the background, theory, and development of conformal transformation as applied to cascades. This Appendix will show the step by step process of the conformal transformation, by means of a sample calculation. The point chosen is the 50% chord station of the upper surface.

NACA Report 824 by Abbott and Von Doenhoff gives the coordinates of the camber line and standard thickness form for this blade. The upper surface, 50% chord position is found by adding the mean camber ordinate, 6.618, to the basic thickness, 4.812, at this point. The result is that the ordinate is 11.43 at station 50, both numbers in per cent chord. Fig. B-1a of this Appendix shows this point plotted on the x' - y' axes. These x' - y' axes are at a 14.1 degree angle of attack. The reason for this angle of attack is discussed in the thesis proper.

In order to use the conformal transformation formulae as developed in Ref. 5, it is necessary to obtain the coordinates of all points referred to the x - y axes of Fig. B-1a. From Fig. B-1a it can be seen that:

$$x = x' \cos\alpha + y' \sin\alpha$$

$$y = y' \cos\alpha - x' \sin\alpha$$

Applying these equations to the point being considered, shows that:

$$x = (50.000)(\cos 14.1^\circ) + (11.430)(\sin 14.1^\circ)$$
$$= 51.27812$$

$$y = (11.430)(\cos 14.1^\circ) - (50.000)(\sin 14.1^\circ)$$
$$= -1.09511$$

For the conformal transformation from rectangular coordinates to circular coordinates such as Fig. B-1b, the author of Ref. 5, on page 10, arrives at the following equations:

1) $R = \frac{r_2}{r_1} = e^{\left(\frac{mx-y}{m^2+1}\right)}$

2) $\Theta = \frac{my+x}{m^2+1}$

where: r_2 = final radius

r_1 = initial radius

e = 2.71828

m = $\tan\beta$

x, y = rectangular coordinates

Θ = circular coordinate (radians)

β = angle of logarithmic spiral with tangential direction.

β in the present case is 15°, while $r_1 = 8.1$ inches.

The authors of the thesis knew they wanted the final blade to extend outward radially a distance of 1.4 inches. This set

$$R = \frac{r_2}{r_1} = \frac{8.1 + 1.4}{8.1} = 1.17283.$$

Then knowing $m = 0.26795$, and $m^2 + 1 = 1.07180$,

as shown in $$1.17283 = e^{\left(\frac{mx-y}{1.07180}\right)}$$

or at station 100,

I) $K(mx-y) = 0.17075$

The values of x and y at station 100 are found in the same way as x and y for the 50% chord station. When the station 100 values of x and y are substituted into equation I), the result is a factor, K, needed for the radial distance desired. All values of x and y are then multiplied by this factor before substitution into equations I) and 2). This factor, K, turned out to be 0.0033913.

Then for the 50% upper chord station,

$$r_2 = (8.1)\, e^{\left(\frac{mx-y}{m^2+1}\right)(0.0033913)}$$

$$= (8.1)\, e^{\left[\frac{(0.26795)(51.278) - (-1.09511)}{1.07180}\right](0.0033913)}$$

$$= 8.489''$$

Θ, in degrees, measured counter-clockwise from the leading edge of the blade is: $\left(\frac{my+x}{m^2+1}\right)(0.0033913)(57.29578)$

$$= \left[\frac{(0.26795)(-1.09511) + 51.278}{1.07180}\right](0.0033913)(57.29578)$$

$$= 9.9068 \text{ degrees.}$$

Therefore, in the circular cascade, the transformed point will have the coordinates:

$$r_2 = 8.489 \text{ inches}$$

$$\theta = 9.987 \text{ degrees},$$

as shown in Fig. B-1b.

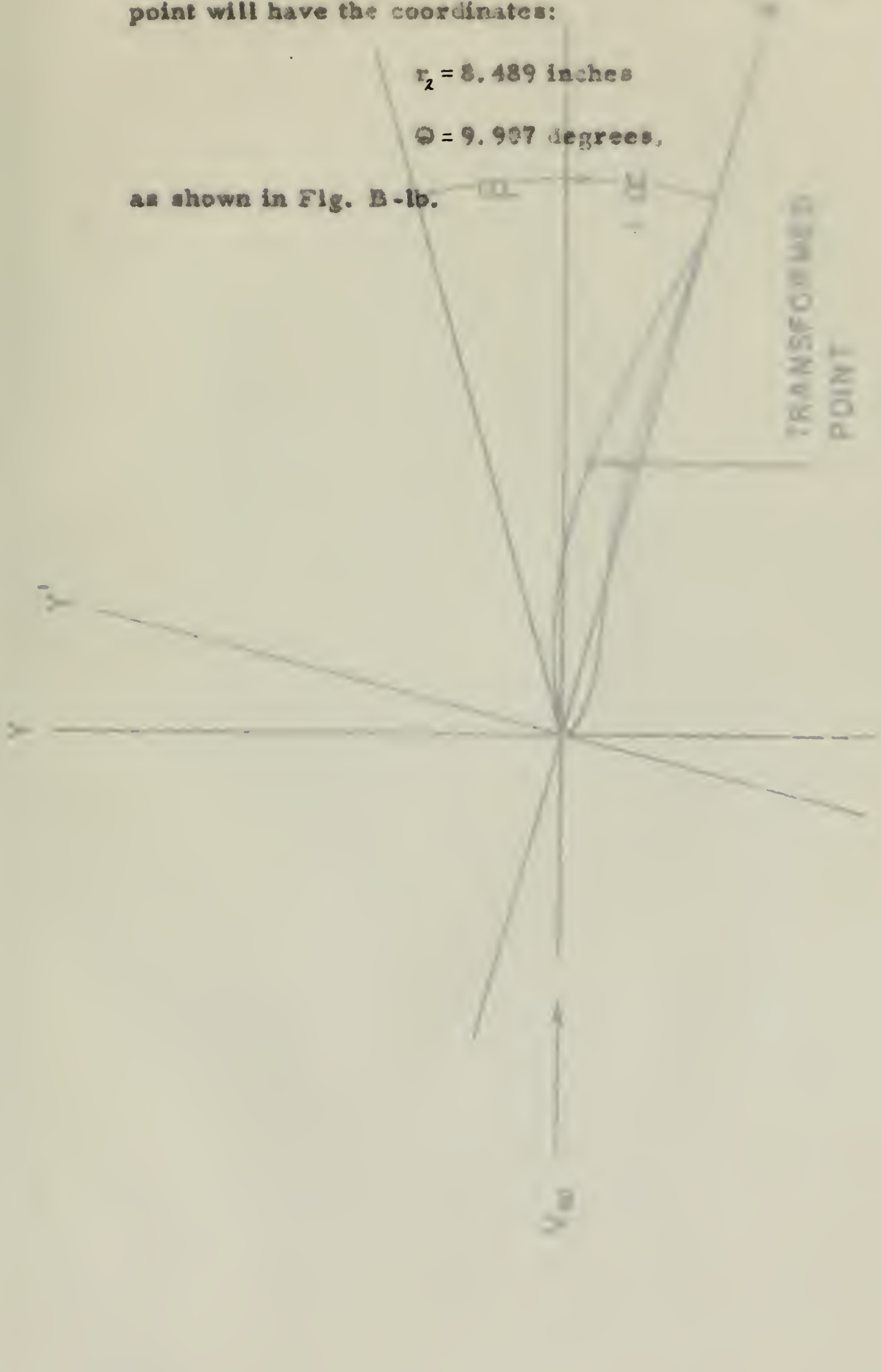

RECTANGULAR COORDINATES FOR CONFORMAL TRANSFORMATION

FIG. B-1a

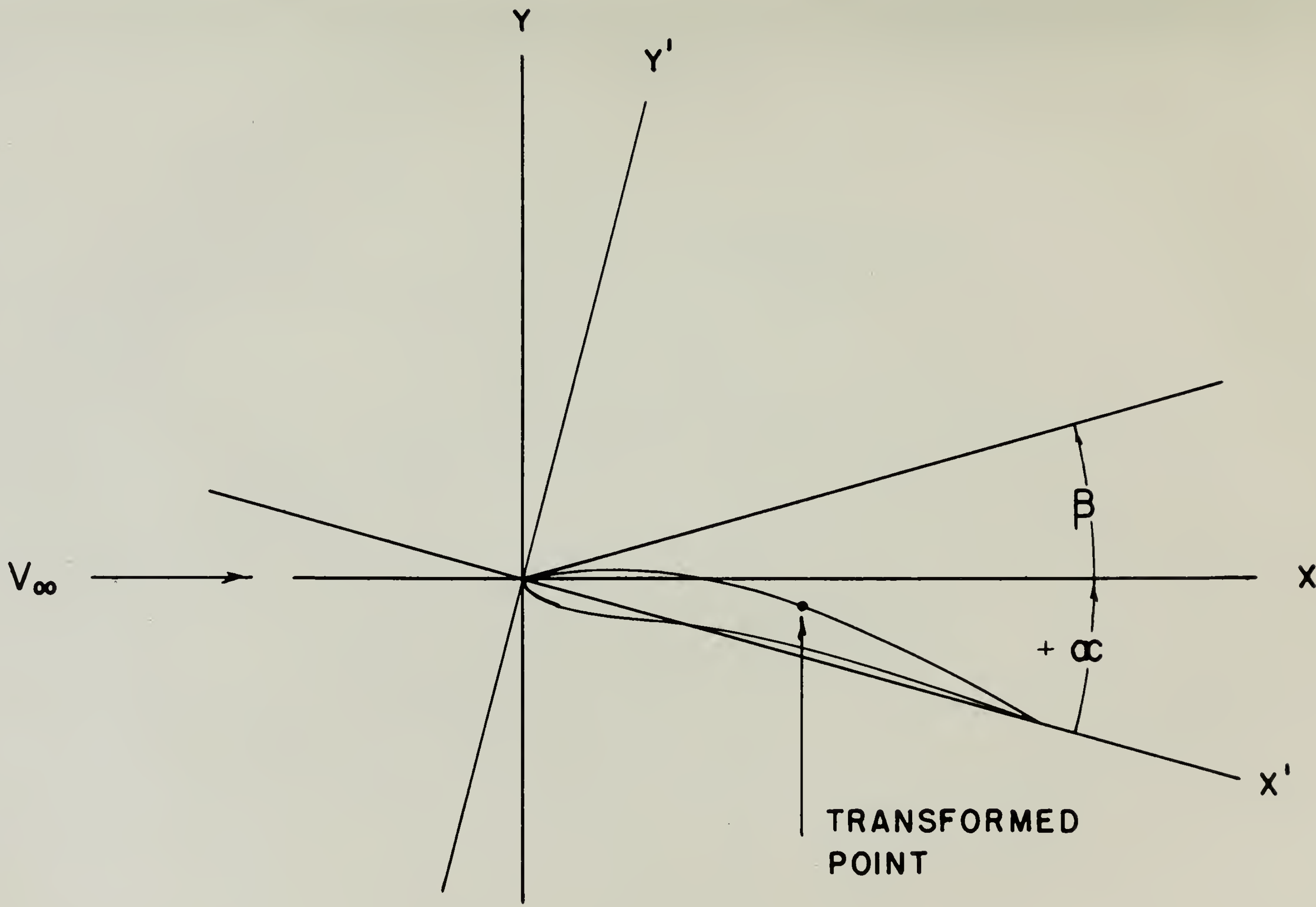

RECTANGULAR COORDINATES FOR
CONFORMAL TRANSFORMATION

FIG. B-1a

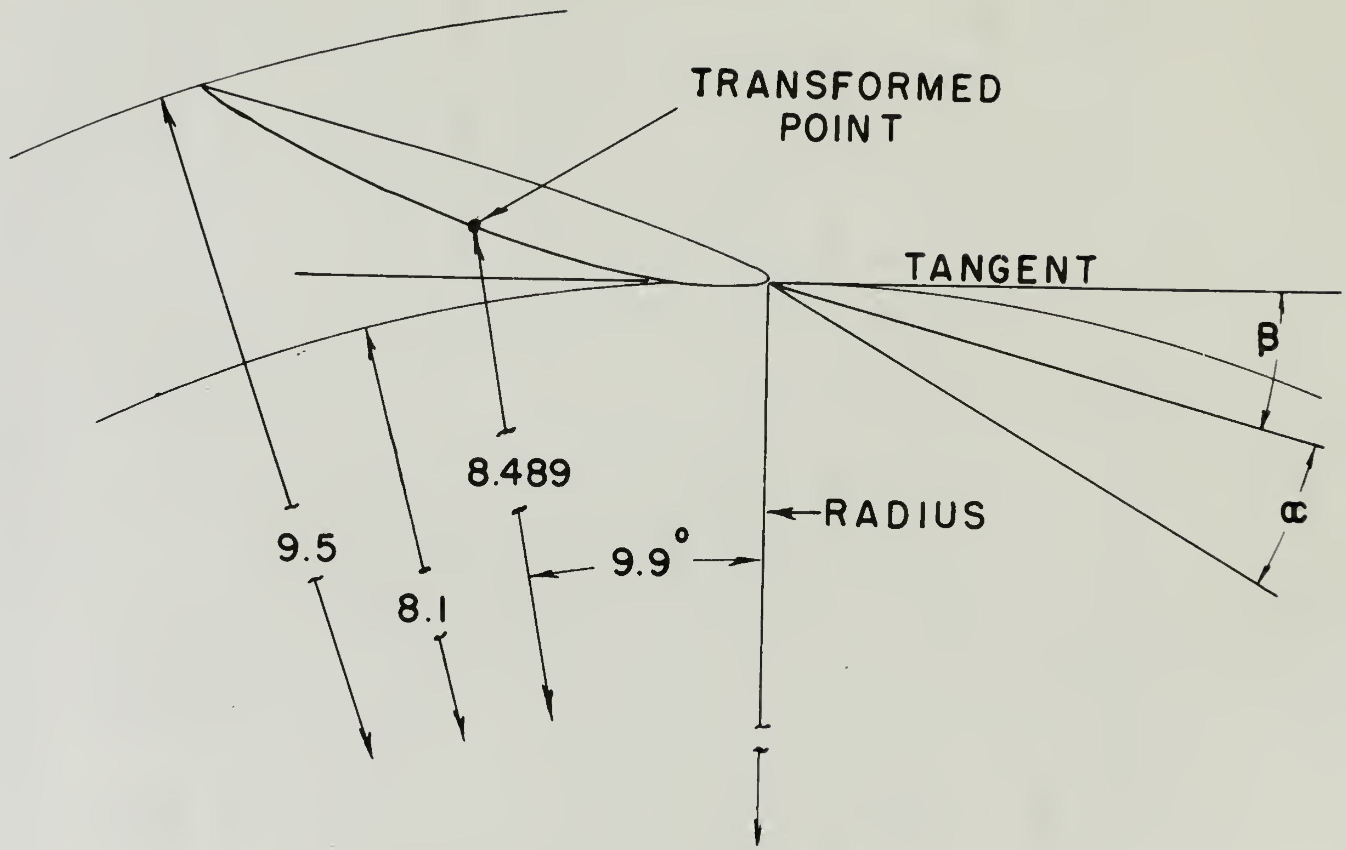

CIRCULAR COORDINATES FOR
CONFORMAL TRANSFORMATION

FIG. B-1b

Appendix C

BARIUM TITANATE CRYSTALS

There was insufficient literature available to learn the capabilities and limitations of the barium titanate crystals which were available. In order to learn these capabilities and limitations, some experiments were undertaken.

One crystal was hooked to an oscilloscope. A quick check showed that the crystal was responsive to whistled or spoken noise, but insensitive to steady blowing. A variable speed electric motor was fitted with a stiff piece of cardboard. This cardboard was circular with a radius of seven inches. It had a one inch slot cut in one side. By placing a fan on one side of the cardboard and the crystal on the other, the range of sensitive frequencies of the crystals could be found. The speed of the cardboard disc was varied. The bottom frequency of response readable on the oscilloscope was approximately five cycles per second. Using musical tones, the crystals responded to 5000 cycles, and apparently would respond to higher frequencies.

Response to musical tones was sufficient proof that the crystals would respond to the changes in pressure due to stall, if that stall occurred faster than five cycles per second. Since

steady pressure measurements were not desired, but pressure fluctuations were, it was decided that these crystals would serve the thesis experiments very well.

After two months of use, some of the crystals started to lose their polarization. Repolarization of the crystals consisted of establishing 110 volts D. C. opposite polarity on each of the two leads, with a ground on the brass clip. The crystals were then heated to 265 degrees Fahrenheit, held there for fifteen minutes and then allowed to cool slowly with the voltage still applied.

Close calibration of the crystals is very difficult. For that reason, they are poor for quantitative measurements, although for qualitative pressure fluctuation measurements they are suitable. Because of their sensitivity, the crystals must be shielded and mounted securely in the test set-up.

Tests were made with the crystals in parallel and it was seen that there was no feedback discernible. Since the crystals could be selected for nearly the same sensitivity, when put in parallel, simultaneous pressure fluctuations on more than one crystal did not add on the oscilloscope. This is because the crystals generate an e.m.f. which is approximately equal.

Appendix D

OPERATING POINT CALCULATIONS

This procedure was followed in determining and setting an operating point. Equations to be used are found on Fig. 11 of the thesis. They are repeated here for convenience:

$$P_r = \frac{P_{02}}{P_{01}}$$

$$\pi_{m_i} = 2.67 \times 10^{-3} \frac{(RPM)}{\sqrt{T_{01}}}$$

The date of the selected run was May 12, 1954. The operating point desired is number 4 of Table I of the thesis -- P_r = 2.20; π_{m_i} = 0.418; MFF = 0.300. Barometric pressure was 30.27 inches of mercury, or 14.83 psia. Room temperature was 74°F. The readings taken were P_{01} (gage), P_{02}(gage), T_{01}, and RPM.

Following the method outlined in the Procedure Section, the compressor was brought up to 3000 RPM. The atmospheric inlet valve to the tunnel was closed.

When steady-state conditions were attained, the following readings were taken:

RPM = 3000, P_{02} = -0.3 psig, P_{01} = -6.8 psig, T_{01} = 65°F

$$P_r = \frac{14.8 - 0.3}{14.8 - 6.8} = 1.815$$

$$\pi_{m_i} = 2.67 \times 10^{-3} \frac{(3000)}{\sqrt{65+460}} = 0.350$$

at this point, MFF = 0.215

As P_r and Π_{m_i} were low, the RPM was raised. As the RPM was increasing, the compressor started to surge. This surging necessitated opening the by-pass valve to keep the actual operating point below the surge line. Conditions steadied down at 3550 RPM. Then the following readings were taken:

RPM = 3550, P_{02} = 3.3 psig, P_{01} = -6.7 psig, $T_{01} = 66^{\circ}F$

$$P_r = \frac{14.8 + 3.3}{14.8 - 6.7} = 2.235$$

$$\Pi_{m_i} = 2.67 \times 10^{-3} \quad \frac{3550}{\sqrt{526}} = 0.415$$

Therefore, MFF =0.295

These values of pressure ratio and mass flow factor were close enough to the desired operating point, to be within the arbitrary limits set in the thesis. These arbitrary limits were:

Pressure ratio =0.05

Mass Flow Factor =0.025

Conditions at the compressor control board were held at the desired operating point while a survey was made at the test section.

28830

H438 Hemler

Investigation of rotating stall in a centrifugal vaned diffuser.